Morphology of Comb-Shaped Proton Exchange Membrane (PEM) Copolymers Based on a Neutron Scattering Study

M-P. Nieh [1], M.D. Guiver [2], D.S. Kim [2], J. Ding [2], and T. Norsten [2]

[1] Canadian Neutron Beam Centre, National Research Council, Chalk River Laboratories, Chalk River, ON, Canada K0J 1J0

[2] Institute for Chemical Process and Environmental Technology, National Research Council Canada, Ottawa, ON, Canada K1A 0R6

Proton exchange membrane (PEM) is a semi-permeable membrane that is designed to conduct protons but is impermeable to gases such as hydrogen and oxygen. For the application to fuel cells, PEM serves an important function to separate reactants and transport protons. Ideal PEM materials should possess properties such as high proton conductivity, high chemical stability over the required temperature range, good mechanical properties and dimensional stability in the hydrated state. Block copolymers forming hydrophobic and interconnected hydrophilic (ionic) domains have many of the aforementioned properties. The hydrophobic matrix provides the mechanical strength and constrains the swelling of the materials, while the hydrophilic (ionic) domains determine the proton conductivity. In order to better design polymer architectures and improve performance of PEM materials, it is essential to resolve their morphologies. In the past, small angle neutron scattering (SANS), X-ray scattering (SAXS) and wide angle X-ray scattering (WAXS) have been powerful tools for structural characterization of PEMs.

Recently, a comb-shaped copolymer has been developed based on a highly fluorinated and rigid polyaromatic backbone containing monodisperse α-methyl polystyrene sulfonic acid side-chains (Figure 1) [1]. The comb-shaped copolymer PEMs exhibit very low hydration-based dimensional changes at elevated operating temperatures with similar proton conductivity and water uptake values compared to the bench-marked PEM, Nafion. We have studied the structures of two comb-shaped copolymers: PEM-19 (19 wt.% side chain content) and PEM-32 (32 wt.% side chain content), which represent the extremes of a low and high ion exchange capacities, having proton conductivities lower (19 wt.%) and higher (32 wt.%) than Nafion, respectively. In this study, we used the following two SANS instruments: NG3 at the National Institute of Standards and Technology (NIST) and E3 at the Canadian Neutron Beam Centre (CNBC).

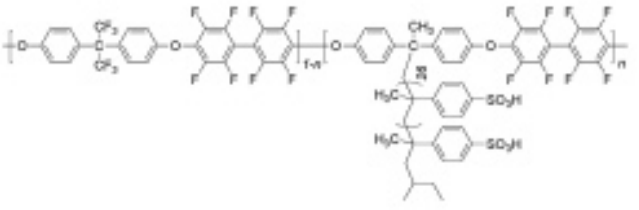

Fig. 1 Molecular structure of comb-shaped copolymer.

The SANS results of D_2O-soaked PEM-19 and PEM-32 as shown in Figure 2, illustrate a similar scattering pattern, presumably resulting from the same morphology. The general feature of both curves is a gradual decay of the intensity over the whole q range with a strong and broad peak at q = 0.03 ~ 0.04 Å^{-1} and a shoulder at q = 0.06 ~ 0.08 Å^{-1}, which could be the second order Bragg peak, followed by another broad peak at higher q between 0.2 and 0.25 Å^{-1}. Comparing these two curves, the low-q peak shifts outwards, corresponding to a smaller length, and the high-q peak shifts inwards with an increased intensity, corresponding to a larger length, when the sample contains more sulfonic acid groups (i.e., PEM-32). Low-q peaks were also observed in other PEM materials and Nafion in the past and interpreted as a "crystalline peak" [2-6]. As for the high-q peak, it is well known through many SANS and SAXS studies on Nafion that there is an "ionomer peak" located around 0.1 ~ 0.25 Å^{-1}, which shifts toward lower q and had an increased intensity at higher hydration levels [1,7-9]. The same trend of shift and intensity and the similar vicinity of the high-q peak observed in our SANS measurement further confirms that it is the "ionomer peak."

Here, we propose an approach to fit the SANS data by focusing on low-q and high-q regimes individually. The scattering intensity in the low q regime is mainly attributed to the crystalline phase composed of large hydrophobic and hydrophilic domains, whereas the high-q scattering mainly comes from the local distribution of the ionomers and water (D_2O) in the hydrophilic domain. Therefore, the scattering function, $I(q)$ can be split into two terms as follows:

1). $$I(q) = I_{crystalline}(q) + I_{ionomer}(q)$$

We assume that the density distribution in the hydrophilic domain could more resemble the case of microemulsions considering the mixing of polyions and water. Therefore, $I_{ionomer}(q)$ can be formulated with the Teubner-Strey model (T-S model) [10], which is derived based on Landau's free energy theory and Debye-Anderson-Brumberger's derivation of scattering by inhomogeneous domains [11], with a correlation function, γ(r) (in Equation 2) yielding a scattering function as Equation 3:

2). $$\gamma(r) = \frac{d}{2\pi r} e^{-r/\xi} \sin\left(\frac{2\pi r}{d}\right)$$, and

3). $$I_{T-S}(q) = \frac{1}{a_2 + c_1 q^2 + c_2 q^4} \quad ,$$

where a_2, c_1, and c_2 are the coefficients of various terms of order parameters in Landau's free energy. In the case of microemulsion, c_1 indicates the tendency of forming interfaces between domains and is usually negative, when a_2 is positive, to favour the formation of microemulsion. A positive c_2 stabilizes the system to meet the criteria of $4a_2c_2 - c_1 > 0$ for a stable morphology.

The T-S scattering function, $I_{T-S}(q)$ describes a morphology of two alternating domains losing long-range order and has a characteristic feature of a low-q plateau with a peak followed by a q^{-4} decay (as shown in Figure 2). Since the intensity of the low-q plateau is simply a flat background for the low-q data, it does not affect the structural parameters of the crystalline phase obtained from the SANS data in this regime. The two length scales, d and ξ, in Equation 2 represent the domain periodicity of the system, which is related to spacing of the domains, and the correlation length of the system, which is related to the decay length of the domains, respectively, and can be related with the coefficients at the denominator of $I_{T-S}(q)$ as expressed below [10]:

4). $$\xi = \left[\frac{1}{2}\left(\frac{a_2}{c_2}\right)^{1/2} + \frac{1}{4}\frac{c_1}{c_2}\right]^{-1/2} \quad \text{,and}$$

$$d = 2\pi\left[\frac{1}{2}\left(\frac{a_2}{c_2}\right)^{1/2} - \frac{1}{4}\frac{c_1}{c_2}\right]^{-1/2} \quad ,$$

The application of T-S model does not require the assumption of aggregates with a regular location or shape and size, such as spheres, ellipsoids, disks, cylinders, yet the ratio, S/V, of the ionomer-water interfacial area (S) to hydrophilic volume (V), can be still obtained through Porod's law:

5). $$\frac{S}{V} = \frac{4\phi_w^{phil}(1-\phi_w^{phil})}{\xi} \quad ,$$

where ϕ_w^{phil} is the volume fraction of water in the hydrophilic domain [10].

Regarding $I_{crystalline}(q)$, to describe the crystalline phase at low-q regime, two different models are employed to fit the SANS data: stacking layered disks (similar to lamellar model with a smaller planar region) and worm-like elongated aggregates with a hard disk structure factor as shown in Figure 3 (see page 86). The best-fit result of stacking layered disks model (the dark grey curve in Figure 2) to the PEM-19 SANS data indicates several mismatching regions compared with the experimental data. First, the fit overestimates the minimum prior to the first order peak and the maximum of the second order peak. Second, the model predicts a sharper decrease after the second order peak. In light of the aforementioned observations, stacking disks may not be the best model to describe the PEM morphology. The other model is the worm-like elongated aggregates model proposed for worm-like micelles is chosen to be the form factor, $F_{WL}(q)$ [12] combining with a hard disk structure factor, $S_{HD}(q)$ to account for the radial interaction among the worm-like cylinders [13]. This is based on the assumption that the radial interparticle interaction among the long aggregates is expected to be much more significant than the axial interaction in the current q-range. Therefore, $I_{crystalline}(q)$ can be expressed as

6). $$I_{crystalline}(q) = \Delta\rho^2\phi_{phob}(1-\phi_{phob})\cdot\bar{\upsilon}\cdot S_{HD}(q)F_{WL}(q)$$

where $\Delta\rho$, ϕ_{phob}, $\bar{\upsilon}$ are the difference of scattering length densities (SLDs) between hydrophilic and hydrophobic domains, the volume fraction of hydrophobic domain and the volume of individual cylindrical aggregates, respectively.

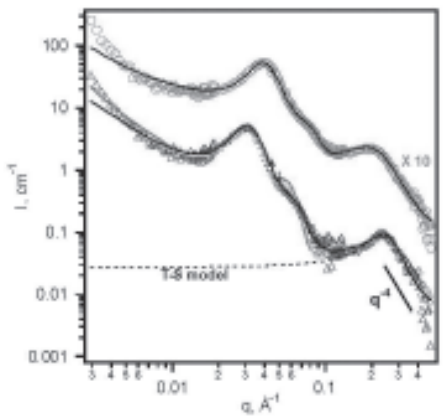

Fig. 2 SANS data for PEM-19 (triangles) and PEM-32 (circles) with best fits of various low-q models: stacking disks (dark grey), flexible cylinders with a circular cross-section (light grey), flexible ellipsoidal cylinders (black). For better clarity, the data of PEM-32 is shifted by a factor of 10 and only fitted with the flexible ellipsoidal cylinder model. In the high q regime, the best-fitting T-S model to PEM-19 SANS data is shown as the dashed line.

The best-fit (the light grey curve in Figure 2) shows a better agreement with the SANS data at maxima and minima than the stacking disks model, except for the minimum after the second order peak. The mismatch is mainly attributed to the unrealistic constraint on the fixed, circular radius of the hydrophilic domain and can be improved by introducing an ellipsoidal cross-section with an aspect ratio at cross-section (the black curve in Figure 2).

The "rocking" curves of both copolymer films were taken at the low-q crystalline peaks as a function of sample angle,

ψ , where ψ = 0 is defined as neutron beam being parallel with the film surface. Both curves are practically flat with no more than a 20% higher intensity at $-2° < \psi < 2°$ than the rest (Figure 4), indicating only slightly preferred orientation, if any, along the surface of the samples for this crystalline phase.

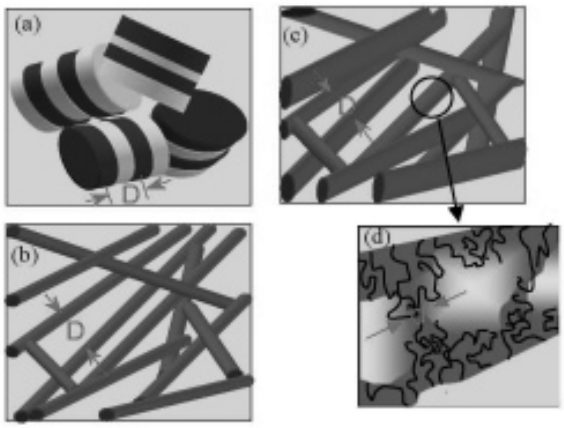

Fig. 3 *Various schemes to explain the morphology of the PEMs. (a) stacking disks model, (b) interconnected flexible circular cylinder model, and (c) interconnected flexible eelipsoidal cylinder (FEC) model. In all cases, the grey represents hydrophobic domains (presumably polymer backbones) and the black represents hydrophilic domains (presumably polymer side-chains and water). The average inter-domain spacing at the crystalline phase, D, yields the crystalline peak. (d) The zoom-in of the hydrophilic domains proposed with the FEC model where hydrophilic side-chains (polystyrene sulfonic acid groups) are depicted as black curves sequestering the hydrophobic-water interface and extending into the water channels. The shading represents the SLD, which is proposed to change gradually from side-chain-rich regions (dark) to water (i.e., D_2O)-rich ionomers (light) with a decay length of ξ (see text) and the average distance among ionomers is d, as described in T-S model.*

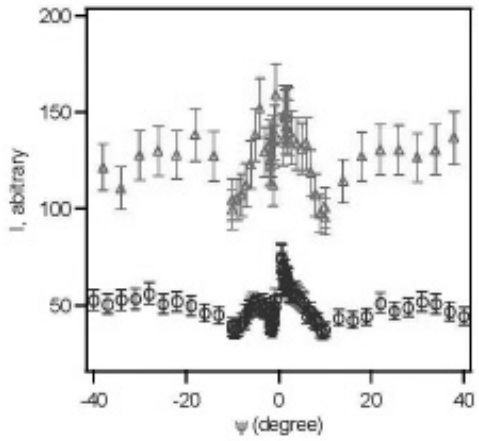

Fig. 4 *Rocking curves of PEM-19 (circles) and PEM-32 (triangles) as a function of sample angle (ψ) at the first order Bragg's peak (crystalline peak).*

In conclusion, the proposed compact FEC with T-S model is able to fit the SANS data nicely in the *q* range from 0.005 to 0.4 $Å^{-1}$ and describes the structure rationally over a large range of length scales. To the best of our knowledge, such agreement between SANS data and model over two decades of *q* values had never been reported previously. Moreover, since only minimal preferential orientation is found along the surface of the film, the worm-like water channels orient more or less isotropically, indicating that the solution casting does not create a situation that defeats the desired property for PEM used in FC, where high proton conductivity is through the film.

References

[1] Norsten, T. B.; Guiver, M. D.; Murphy, J.; Astill, T.; Navessin, T.; Holdcroft, S.; Frankamp, B.L.; Rotello, V. M.; Ding, J. Adv. Funct. Mat. 2006, 16:1814-1822.

[2] Kim, M.-H.; Glinka, J. C.; Grot, S. A.; Grot, W. G. Macromolecules 2006, 39:4775-4787.

[3] Mauritz, K. A.; Moore, R. B. Chem. Rev. 2004, 104:4535-4585.

[4] Gebel, G.; Diat, O. Fuel Cells 2005, 5:261-276.

[5] Rubatat, L.; Shi, Z.; Diat, O.; Holdcroft, S.; Frisken, B. J. Macromolecules 2006, 39:720-730.

[6] Kim, J.; Kim, B.; Jung, B. J. Membr. Sci. 2002, 207:129-137.

[7] Gierke, T. D.; Munn, G. E.; Wilson, F. C. J. Polym. Sci.: Polym. Phys. Ed. 1981, 19:1687-1704.

[8] Fujimura, M.; Hashimoto, T.; Kawai H. Macromolecules 1981, 14:1309-1315.

[9] Dreyfus B.; Gebel, G.; Aldebert, P.; Pineri, M.; Escoubes, M.; Thomas, M. J. Phys. (France) 1990, 51:1341-1354.

[10] Teubner, M.; Strey, R. J. Chem. Phys. 1987, 87:3195-3200.

[11] Debye, P.; Anderson, H. R.; Brumberger, H. J. Appl. Phys. 1957, 28:679-683.

[12] Chen, W.-R.; Butler, P. D.; Magid L. J. Langmuir 2006, 22:6539-6548.

[13] Rosenfeld, Y. Phys. Rev. A 1990, 42:5978-5989.